ISSN 1063-7834, Physics of the Solid State, 2008, Vol. 50, No. 3, pp. 511–514. © Pleiades Publishing, Ltd., 2008.
Original Russian Text © S.V. Mel'nikova, N.M. Laptash, 2008, published in Fizika Tverdogo Tela, 2008, Vol. 50, No. 3, pp. 493–496.

LATTICE DYNAMICS AND PHASE TRANSITIONS

Phase Transitions in Orthorhombic Oxyfluoride $(NH_4)_2MoO_2F_4$

S. V. Mel'nikova[a] and N. M. Laptash[b]

[a] *Kirensky Institute of Physics, Siberian Branch, Russian Academy of Sciences, Akademgorodok, Krasnoyarsk, 660036 Russia*
e-mail: msv@iph.krasn.ru

[b] *Institute of Chemistry, Far East Division, Russian Academy of Sciences, pr. Stoletiya Vladivostoka 159, Vladivostok, 690022 Russia*
e-mail: laptash@icp.dvo.ru

Received June 25, 2007

Abstract—$(NH_4)_2MoO_2F_4$ single crystals were grown and studied using polarization-optical methods, and the birefringence was measured in the temperature range 90–350 K. The following sequence of phase transitions is revealed: $G_0 \rightleftarrows G_1 \rightleftarrows G_2$. It is established that the phase transition at $T_{01} \approx 267$ K is of the first order and exhibits thermal hysteresis $\delta T_{01} \approx 0.6$ K. A weak anomaly is found in $\Delta n(T)$ at $T_{02} \approx 180$ K. The crystals are shown to retain the orthorhombic symmetry during the phase transitions.

PACS numbers: 61.66.Fn, 77.80.Bh, 78.20.Fm

DOI: 10.1134/S1063783408030207

The polar noncentrosymmetric oxyfluoride anions $MO_xF_{6-x}^{n-}$ (M = Nb, Mo, W; x = 1, 2, 3) are potentially good building blocks for creating polar structures exhibiting a number of valuable physical properties (pyro-, ferro-, and piezoelectricity; optical second harmonic generation) [1]. Their position in a noncentrosymmetric crystal lattice can prevent the dipole moments of individual octahedra from being neutralized [2]. However, in actual practice, many (if not most of) oxyfluoride compounds of transition metals containing these polar anions are orientationally disordered and are characterized by complete oxide/fluoride disordering and the absence of resulting polarity [1]. The members of the relatively large family of disordered nonpolar oxyfluorides $A_2BMO_3F_3$ (A, B = K, Rb, Tl, Cs, NH_4; M = Mo, W) containing a locally polar pseudo-octahedral unit crystallize in the elpasolite structure (cubic symmetry, space group $Fm\bar{3}m$, the number of molecules in the unit cell Z = 4). As the temperature decreases, they undergo ferroelectric or ferroelastic phase transitions (PTs) associated with ordering of the anion sublattice [3]. The size of the central atom M in the octahedron substantially influences the temperature of the transition from the cubic phase. In the molybdenum-containing compounds, the transition occurs at a temperature 50 to 70 K higher than that in the tungstates [3–5].

In this work, we analyze PTs occurring in the molybdenum and tungsten oxyfluorides $(NH_4)_2MoO_2F_4$ and $(NH_4)_2WO_2F_4$.

According to [6], $(NH_4)_2WO_2F_4$ crystallizes in the orthorhombic system (space group $Cmcm$, Z = 4); a = 5.952(1) Å, b = 14.441(1) Å, and c = 7.157(1) Å. One O2 ion and three fluorine ions in the equatorial plane of the octahedron are disordered. The disorder in this crystal is dynamic and associated with reorientation of the WO_2F_4 octahedra around the fourfold pseudoaxis [7]. Recently [8, 9], a first-order structural PT has been revealed in this crystal at a temperature T_{01} = 202 K with thermal hysteresis $\delta T_{01} \approx$ 6–12 K. This PT is accompanied by twinning and a change in symmetry ($Cmcm \rightleftarrows \bar{1}$). An additional weak anomaly in the DSM signal was found at $T_{02} \approx$ 170 K. The total thermal effect of both anomalies is $\Sigma\Delta H_i = 3200 \pm 400$ J/mol and $\Sigma\Delta S_i = 16.5 \pm 2.0$ J/mol K. The phase transition at T_{01} was referred to the order–disorder type. The anomalies in the birefringence and heat capacity observed at $T_{02} \approx$ 170 K are associated with additional reorientation in the tetrahedral complex.

The ammonium molybdenum oxyfluoride $(NH_4)_2MoO_2F_4$ is the main product of the interaction between initial molybdenum oxide compounds (trioxide MoO_3 or ammonium paramolybdate $(NH_4)_2Mo_7O_{24} \cdot 4H_2O$) with ammonium hydrodifluoride NH_4HF_2 [10–12]. This compound was first described in 1867 [13], but data on its crystal structure are not available in the literature.

We performed polarization-optical studies and determined the birefringence of the $(NH_4)_2MoO_2F_4$ crystal over a wide temperature range with the aim of searching PTs in this crystal and performing a tentative study of them. The birefringence was measured on (001)-, (010)-, and (100)-cut plates using the Berec compensator method with an accuracy of $\approx 10^{-5}$ and the

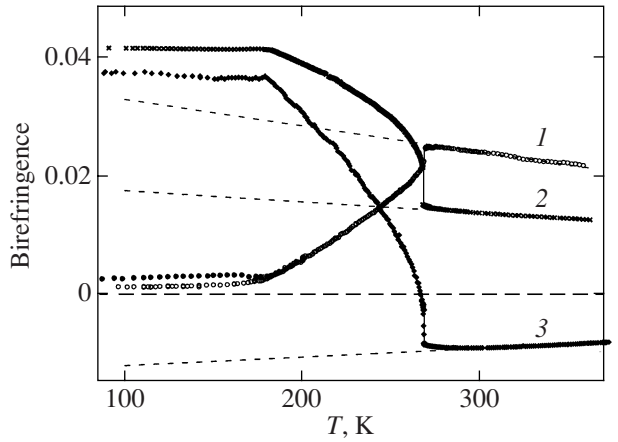

Fig. 1. Temperature dependence of the birefringence in $(NH_4)_2MoO_2F_4$: (*1*) Δn_a, (*2*) Δn_b, and (*3*) Δn_c.

Senarmont compensator method with a sensitivity higher than $\approx 10^{-7}$ at a wavelength of 6328 Å. The former method was used to determine the magnitude of the measured quantity, and the latter allowed us to study its temperature dependence. All the experiments were carried out over the temperature range from 90 to 350 K. Polarization-optical and crystal-optical observations and measurements of the refractive indices were performed using an Axiolab polarizing microscope.

To grow bulk $(NH_4)_2MoO_2F_4$ single crystals, we used, as the starting material, $(NH_4)_3MoO_3F_3$ obtained as a product of the reaction between an ammonium molybdate solution and a concentrated (40%) NH_4F solution with the formation of abundant white sediment. The molybdate can easily be obtained by simply dissolving molybdenum trioxide in ammonia. In addition to $(NH_4)_3MoO_3F_3$, the white sediment can also contain $(NH_4)_2MoO_3F_2$ as an impurity. Both of these compounds are easily soluble in HF with the formation of an aqueous solution of $(NH_4)_2MoO_2F_4$:

$$(NH_4)_3MoO_3F_3 + HF = (NH_4)_2MoO_2F_4 + NH_3 + H_2O,$$

$$(NH_4)_2MoO_3F_2 + 2HF = (NH_4)_2MoO_2F_4 + H_2O.$$

As a result of slow evaporation of the solution in air, large $(NH_4)_2MoO_2F_4$ single crystals are formed in the shape of prisms or thick plates. The x-ray powder diffraction patterns of these crystals at room temperature were found to be identical with small differences in the magnitudes of the unit cell parameters.

The grown crystals are similar in shape to $(NH_4)_2WO_2F_4$ crystals [8] but differ from them in terms of the orientation of the unit cell axes with respect to the crystal faces. The smallest dimension of the $(NH_4)_2MoO_2F_4$ single crystals is along the [010] crystallographic direction ($b = 14.486$ Å). The smallest unit cell parameter is along the crystal length ($a = 5.966$ Å), and the intermediate dimension of the prism is along the [001] direction ($c = 7.112$ Å). The crystals have perfect (010) cleavage plane, which severely hampered the preparation of thin plates of cross-section cuts.

The polarization-optical studies showed that, at room temperature, the $(NH_4)_2MoO_2F_4$ plates cut along the principal crystallographic directions demonstrate a uniform parallel extinction typical of orthorhombic symmetry. However, the refractive-index ellipsoid (optical indicatrix) differs in shape from that in the tungsten compound; namely, the optical-axis plane coincides with (100) and the angle between the optical axes is close to 90°. The relations between the refractive indices are as follows: $n_c = n_g \approx 1.59$, $n_a = n_m \approx 1.57$, and $n_b = n_p \approx 1.56$. The ellipsoid shape corresponds to an optically positive crystal. At low temperatures (100 K), the indicatrix changes in shape and the crystal becomes optically negative. The orientation of the optical-axis plane changes to (010), the acute-angle bisectrix is observed in the [100] direction, and the relationship between the refractive indices is changed: $n_c = n_g$, $n_b = n_m$, and $n_a = n_p$.

Figure 1 shows the measured temperature dependences of the birefringence Δn_a, Δn_b, and Δn_c of the $(NH_4)_2MoO_2F_4$ crystal. The crystal exhibits high anisotropy of the refractive indices and, therefore, becomes a strongly birefringent material. At room temperature, the highest birefringence ($\Delta n_a = 0.023$) is observed in the [100] direction and the lowest in the [001] direction ($\Delta n_c = 0.009$). For light propagating along the [010] direction, the birefringence is $\Delta n_b = 0.014$. The temperature dependence of the birefringence is linear over the temperature range 370–280 K and deviates slightly from the linear behavior at lower temperatures. At 267 K, an abrupt jump in the birefringence is observed. During further cooling, the birefringence in the [010] direction increases smoothly and reaches saturation at 170 K ($\Delta n_b \approx 0.041$). In the [100] direction, the birefringence also decreases smoothly to $\Delta n_a = 0.0011$–0.0015. The greatest changes in the birefringence are observed for light propagating along the [001] direction; specifically, the optical anisotropy decreases abruptly almost to zero near the PT point and then it changes sign and increases smoothly as the temperature decreases. Near $T \approx 180$ K, the $\Delta n(T)$ dependence exhibits a sharp change in slope (Fig. 1). Moreover, at this temperature, the observation conditions are substantially changed. Indeed, at $T > 180$ K, these conditions are good: clear compensation, narrow lines, and good repeatability. Below 170 K, the observation conditions are sharply impaired and the data are not repeated upon next cycles of measurement. This fact is illustrated in Fig. 1 through the example of the $\Delta n_a(T)$ dependence, where filled and open circles correspond to different cycles of measurement.

The dashed lines in Fig. 1 show the temperature dependence of the birefringence extrapolated from the initial phase. It is seen that, in the crystal studied, the temperature dependence is strictly linear over a wide

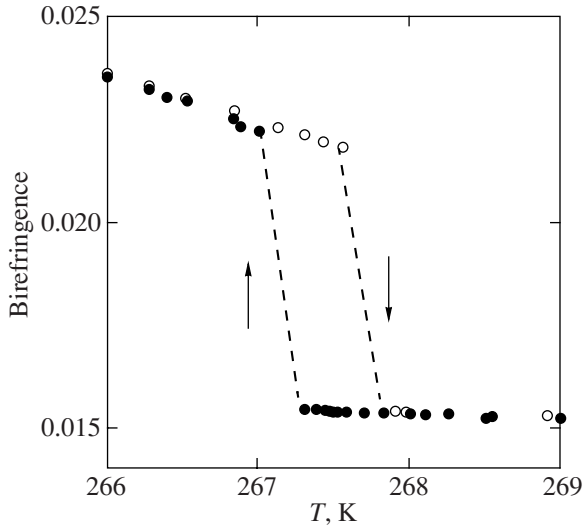

Fig. 2. Behavior of the birefringence $\Delta n_b(T)$ near T_{01}.

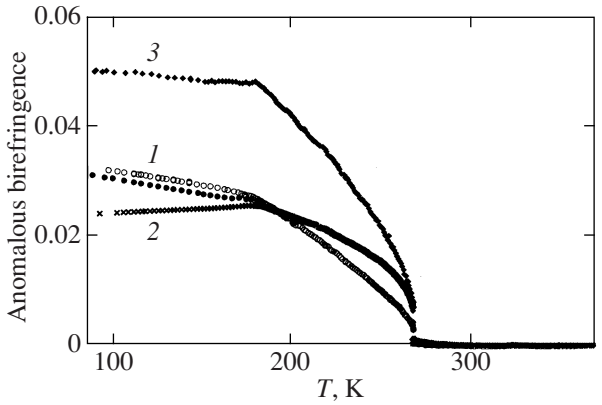

Fig. 3. Temperature dependence of the anomalous portion of the birefringence in the $(NH_4)_2MoO_2F_4$ crystal: (*1*) Δn_a, (*2*) Δn_b, and (*3*) Δn_c.

temperature range above the PT. Below $T \approx 267$ K, the PT occurs, which is accompanied by a jumpwise change in birefringence and thermal hysteresis $\delta T_{01} \approx 0.6$ K (Fig. 2). On cooling, the PT temperature is $T_{01\downarrow} = 267.2$ K and, on heating, $T_{01\uparrow} = 267.8$ K.

From polarized-light observations on crystalline samples with different thicknesses, it was established that, over the entire temperature range studied, the (100)-, (010)-, and (001)-cut plates demonstrate uniform parallel extinction and no twins are seen. The change in the sigh of the birefringence along the [001] axis is accompanied by the appearance, changes, and disappearance of interference colors slightly below the transition point T_{01}. Below 180 K, an interference color indicating weak optical anisotropy is seen along the [100] axis, where the optical anisotropy was observed to be the largest at room temperature.

Figure 3 shows the anomalous portion of the birefringence, $\delta n(T)$, which is defined as the deviation of the measured birefringence from the extrapolated linear dependence (Fig. 1). It is seen that, in contrast to the tungstate [8], pretransition phenomena are manifested only slightly here. The anomalous portion of the birefringence appears in a jumpwise manner at T_{01} and is about 10% of the maximum value; then, it increases smoothly. Near 180 K, the slope of the curve is changed. Thus, the temperature range studied can be divided into three parts: one part corresponds to the initial orthorhombic phase G_0 and two other parts correspond to phases G_1 (267–180 K) and G_2 (below 180 K). The temperature dependence of the birefringence in the G_1 phase is well described by the Landau theory for first-order PTs near a tricritical point. As is shown in [14], in quantitative calculations of the anomalies in physical properties, it is necessary to take into account the sixth-order term in an expansion of the thermodynamic potential. In this case, for $\delta n \sim \eta^2$, the linear dependence $[\delta n - (2/3)\delta n_0]^2 \sim (T_{01} - T)$ should be valid. Here, δn_0 is the jump in the birefringence upon the PT and η is the order parameter. It follows from Fig. 4 that the PT in $(NH_4)_2MoO_2F_4$ is close to the tricritical point; indeed, in the G_1 phase, all experimental points fall on straight lines *1–3* and $T_{cr} - T_{01} \approx 0.4$ K.

Despite the apparent similarity between the $\Delta n(T)$ temperature dependences for molybdate (Fig. 1) and tungstate [8] (first-order PTs, which are accompanied by a jumpwise change in the birefringence), these crystals are different in many respects. First, these crystals differ in terms of the shape of the optical indicatrix even at room temperature, which indicates possible small differences between the structures of these materials. Second, in $(NH_4)_2WO_2F_4$, over a wide temperature range above the PT, strong pretransition "tails" of birefringence are observed, whose magnitude can be as large as 30% of the jump at T_{01}. These tails are charac-

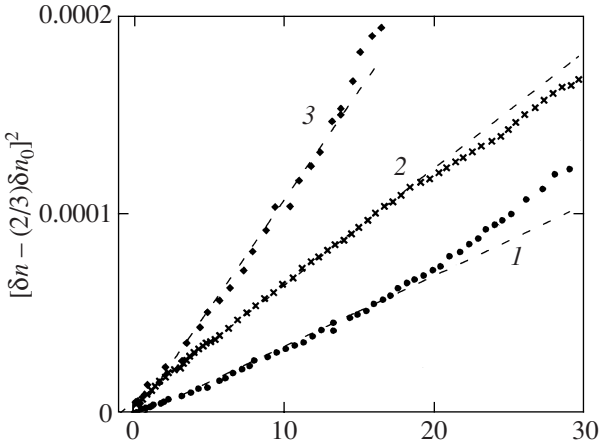

Fig. 4. Temperature dependence of the square of the anomalous portion of the birefringence in $(NH_4)_2MoO_2F_4$: (*1*) Δn_a, (*2*) Δn_b, and (*3*) Δn_c.

teristic of order–disorder PTs and indicate a substantial ordering of the structural elements as a result of the PT [9]. In the molybdate, the $\Delta n(T)$ dependence is strictly linear in the initial phase down to the PT temperature (Fig. 1). This fact demonstrates that the phase transition at T_{01} is associated with shifts of structural elements.

The most significant difference between these crystals is that the crystal system to which the tungstate belongs is changed during the phase transition at T_{01} ($Cmcm \rightleftarrows \bar{1}$); a spontaneous shear strain arises, and the transition is ferroelectric. The crystal is divided into optically distinguishable twins. In $(NH_4)_2MoO_2F_4$, such twins were not detected below T_{01}, which indicates that the crystal most likely retains its orthorhombic symmetry. Moreover, these crystals show absolutely different temperature dependences of the birefringence along the [100] and [010] axes below the PT point. In $(NH_4)_2MoO_2F_4$, the birefringence along [100] decreases abruptly below T_{01}, whereas in the tungsten compound it increases jumpwise. Along the [010] axis, $\Delta n_b(T)$ increases abruptly in the molybdate, whereas in the tungstate it decreases. All of these facts indicate that these crystals differ in symmetry in phase G_1 and in the nature of the PT at T_{01}. It is reasonable to assume that, upon the PT, the $(NH_4)_2MoO_2F_4$ crystal either losses the center of inversion and undergoes the $mmm \rightleftarrows mm2(222)$ transformation or demonstrates a change in translation symmetry without a change in the point group. In the former case, this crystal can be ferroelectric below T_{01}.

Both crystals exhibit similar anomalies of birefringence in the temperature range 170–180 K. Namely, these are slight discontinuities in the slope of $\Delta n(T)$ curves, which are accompanied by impaired experimental conditions and instability of measurements in phase G_3.

The PT temperature of the $(NH_4)_2MoO_2F_4$ crystal is 65 K higher than that of the isomorphous tungstate [8]. Thus, orthorhombic ammonium crystals $A_2MO_2F_4$ demonstrate the same regularity as do elpasolites [3–5]. Despite the small differences between the ionic radii of molybdenum (0.6 Å) and tungsten (0.59 Å), the PT temperatures differ significantly. It is reasonable to assume [15] that the increased M–O bond covalency upon the W $\rightleftarrows$ Mo substitution can influence the PT temperature in oxyfluorides. This factor can also be the reason for the difference between the symmetries of distorted phases.

Thus, we have studied the $(NH_4)_2MoO_2F_4$ compound and found two temperatures at which the $\Delta n(T)$ dependences undergo anomalies. At $T_{01} \approx 267$ K, a phase transition (PT) occurs, which is accompanied by a discontinuous change in the birefringence and thermal hysteresis $\delta T_{01} \approx 0.6$ K typical of first-order PTs. The temperature dependence of the birefringence in the G_1 phase is well described by the Landau theory for first-order PTs near a tricritical point, and it has been found that $(T_{cr} - T_{01}) \approx 0.4$ K. The phase transition at 180 K is accompanied by a slight anomaly of $\Delta n(T)$, and the G_2 phase is characterized by an instability of measurements and impaired experimental conditions. Upon the PT, the crystal retains its orthorhombic symmetry.

ACKNOWLEDGMENTS

The authors are grateful to A.D. Vasil'ev for providing the data on the crystal unit cell parameters at room temperature.

This work was supported by the Council on Grants from the President of the Russian Federation (grant NSh-4137.2006.2) and the Russian Foundation for Basic Research (project no. 08-02-00091).

REFERENCES

1. R. L. Withers, F. J. Brink, Y. Liu, and L. Noren, Polyhedron **26**, 290 (2007).
2. P. A. Maggard, S. N. Tiffany, C. L. Stern, and K. R. Poeppelmeier, J. Solid State Chem. **175**, 27 (2003).
3. J. Ravez, G. Pereudeau, H. Arend, S. C. Abrahams, and P. Hagenmüller, Ferroelectrics **26**, 767 (1980).
4. I. N. Flerov, M. V. Gorev, V. D. Fokina, A. F. Bovina, M. S. Molokeev, Yu. V. Boĭko, V. N. Voronov, and A. G. Kocharova, Fiz. Tverd. Tela (St. Petersburg) **48** (1), 99 (2006) [Phys. Solid State **48** (1), 106 (2006)].
5. I. N. Flerov, M. V. Gorev, V. D. Fokina, A. F. Bovina, M. S. Molokeev, E. I. Pogorel'tsev, and N. M. Laptash, Fiz. Tverd. Tela (St. Petersburg) **49** (1), 136 (2007) [Phys. Solid State **49** (1), 141 (2007)].
6. N. M. Laptash, A. A. Udovenko, A. B. Slobodyuk, and V. Ya. Kavun, in *Abstracts of the 14th European Symposium on Fluorine Chemistry, Poznan, Poland, 2004* (Poznan, 2004), p. 253.
7. E. I. Voit, A. V. Voit, A. A. Mashkovskii, N. M. Laptash, and V. Ya. Kavun, Zh. Struct. Khim. **47** (4), 661 (2006) [J. Struct. Chem. **47** (4), 642 (2006)].
8. S. V. Mel'nikova, V. D. Fokina, and N. M. Laptash, Fiz. Tverd. Tela (St. Petersburg) **48** (1), 110 (2006) [Phys. Solid State **48** (1), 117 (2006)].
9. I. N. Flerov, V. D. Fokina, M. V. Gorev, A. D. Vasiliev, A. F. Bovina, M. S. Molokeev, A. G. Kocharova, and N. M. Laptash, Fiz. Tverd. Tela (St. Petersburg) **48** (4), 711 (2006) [Phys. Solid State **48** (4), 759 (2006)].
10. L. K. Marinina, E. G. Rakov, V. D. Bratishko, B. V. Gromov, and S. A. Kokanov. Zh. Neorg. Khim. **15**, 3279 (1970).
11. G. Pausewang, Z. Naturforsch., B: Anorg. Chem., Org. Chem., Biochem., Biophys., Biol. **26B**, 1218 (1971).
12. L. K. Marinina, E. G. Rakov, B. V. Gromov, B. V. Minaev, and S. A. Kokanov, Tr. Mosk. Khim.-Tekhnol. Inst. im. D. I. Mendeleeva **67**, 83 (1970).
13. D. Delafontaine, Arch. Phys. Nat. **30**, 232 (1867).
14. S. V. Mel'nikova, A. T. Anistratov, and K. S. Aleksandrov, Fiz. Tverd. Tela (Leningrad) **23** (1), 246 (1981) [Sov. Phys. Solid State **23** (1), 138 (1981)].
15. G. Peraudeau, J. Ravez, P. Hagenmuller, and H. Arend, Solid State Commun. **27**, 591 (1978).

Translated by Yu. Ryzhkov